EPJ Web of Conferences **6**, 02002 (2010)
DOI:10.1051/epjconf/20100602002

Impact properties of the aircraft cast aluminium alloy Al-7Si-0.6Mg (A357)

Nikolaos D. Alexopoulos[a]
University of the Aegean, Department of Financial Engineering, 821 00 Chios, Greece

Abstract. The impact mechanical properties of the widely used in the aeronautics A357 cast aluminum alloy were investigated by exploiting experiments on an instrumented Charpy impact testing machine. The evaluated impact properties for 25 different artificial aging heat treatment conditions were analyzed and discussed in conjunction with the respective tensile properties. Correlations are proposed to establish useful relationships between impact resistance and tensile strain energy density properties. The established correlations, which are well supported by the performed experiments, can be used to estimate the tensile ductility and toughness of the A357 cast aluminum alloy from the Charpy impact test. Performed fractographic analyses were supporting the physically arbitrary correlation between tensile strain energy density and impact resistance.

1 Introduction

Precision casting is currently attracting considerable attention as a reliable manufacturing process for producing aeronautical and automotive aluminum components of complex shape geometries cost efficiently. Inferior mechanical properties, specifically in terms of ductility and toughness, and increased scatter compared to the respective wrought aluminum alloys, represent serious drawbacks for their increased exploitation in aeronautical applications. The tighter controls currently applied during the casting process, as well as the advancements on the casting processes and the better understanding of the physical metallurgy background of the age-hardened aluminum alloys led to an improvement of the material quality and, hence, to an appreciable increase of the competitiveness of aluminum casting products [1]. The most widely used alloy for the above applications is the precipitation-hardened Al-7Si-0.7Mg (A357) cast alloy.

The characterization of the quality of a cast alloy involves non-destructive inspection, quantitative metallography and mechanical testing, e.g. [2,3]. Hardness, tensile and impact testing are in principal used to characterize the quality of a cast aluminum alloy in terms of mechanical performance. The demands for increased damage tolerance abilities of cast aluminum alloys have made fracture and tensile toughness important properties. The material property fracture toughness is quite underestimated for the case of cast aluminum alloys. The fracture toughness test, due to its complexity, is usually not performed to cast aluminum alloys and more 'fast' tests, e.g. hardness and tension test are performed to evaluate the mechanical performance of these alloys. Notice that in aircraft and automotive industry, certain minimum values in tensile strength, ductility and fracture

[a] Corresponding author, e-mail: nalexop@tee.gr

toughness are prerequisite for considering a material as a candidate for structural applications. e.g. [4]. Empirical and analytical correlations had been proposed in the literature to calculate or estimate the fracture toughness of several materials from easy to perform tests, such as the impact or the tension test.

In the early 70's the empirical equation (1) was proposed by Barson and Rolfe [5], for both, low-alloyed and austenitic steels to calculate the alloy's plane strain fracture toughness K_{Ic} for known Charpy V-notch impact energy W_{CVN} and yield strength R_p values:

$$\left(\frac{K_{Ic}}{R_p}\right)^2 = m \cdot \left(\frac{W_{CVN}}{R_p}\right)^2 + n \quad . \tag{1}$$

The m and n coefficients are both, empirical and material dependent constants. However, the correlation of the material's fracture toughness and impact energy has not been reported on the open literature for aluminum alloys.

In the present work, the impact properties of the cast aluminium alloy A357 will be evaluated. A direct comparison between the derived impact properties and the already evaluated tensile properties for the same artificial aging conditions will be attempted. The evaluated material property impact resistance R_{CVN} will be empirically correlated to the material's strain energy density W, which is calculated as the integral of the tensile flow curve. According to the literature [6], strain energy density W is proportional to K_{Ic}^2, thus this substitution in eqn.(1) will provide a correlation to fast estimate tensile mechanical properties from the 'simple' Charpy impact test. Fractographic analyses by using a scanning electron microscope will be employed to support the physically arbitrary correlation between tensile strain energy density and impact resistance.

2 Experimental Procedure

The material used for the investigations was A357 aluminum alloy cast ingots. The ingots were supplied by Pechiney, France and were cast with continuous casting process and delivered in form of rods. The use of ingots instead of cast material has been preferred to keep imperfections such as porosity and other inclusions minimal and, hence, to reduce deviations in mechanical properties. The chemical composition of the delivered ingot material was Al-7.0Si-0.55Mg-0.10Ti-0.12Fe-<0.10Mn.

For the experimental investigation, specimens for microstructure characterization, hardness measurements, tensile tests (ASTM E8) and Charpy impact tests (ASTM E23) were cut from the middle section of the ingots to obtain the same solidification conditions. All specimens were solution heat treated for 22 hours at 540^{o}C and quenched in water <10^{o}C, as proposed in [4]. Artificial aging of the specimens was made at the temperatures 155, 175 and 205^{o}C which cover the range of temperatures involved for artificial aging of commercial A357 cast alloys, [7,8].

The cast aluminum alloys were experimentally evaluated by performing tensile and impact tests as well as fractographic analyses for both, tensile and impact specimens. Details about the tensile experiments, the hardness measurements and the metallographic analyses of as cast as well as heat-treated alloys can be found in [9]. For the impact tests, full size Charpy V notch 10 x 10 x 55 mm impact specimens according to ASTM E23 were used. The tests were carried out on an Instron Wolpert instrumented impact-testing machine with maximum dynamic force of 40 kN, controlled by a computer. For each artificial aging condition at least six impact specimens were tested to get an average data point. In total 159 impact tests were performed. To characterize the predominant fracture mechanisms of the investigated tensile and impact test specimens, fracture surface analyses were made. For the fracture surface analyses a Phillips FEG/SEM XL40 scanning electron microscope, with an operating voltage of 20 kV equipped with an EDX system, was used.

3 Mechanical Test Results

The results from tensile tests, hardness measurements as well as metallographic analyses of as cast and heat-treated alloys had been presented and discussed in detail in [9]. Briefly, the performed hardness measurements and metallographic analyses have shown that for artificial aging at 205°C, the peak-aging condition of the alloy was reached after 8 hours. At aging times higher than 16 hours, the overaging condition was observed. At 175°C, for the investigated aging time range up to 48 hours, no indications of overaging were observed. Peak-aging condition at 175°C was observed at aging times lying between 20 and 48 hours. At 155°C, hardness and strength did not reach peak values within the investigated aging time range of 48 hours. As the material's strength increases with the increasing artificial aging time, it is expected that the tensile ductility will decrease [7,8]. Typical engineering tensile stress-strain curves for different artificial aging times can be seen in Figure 1.

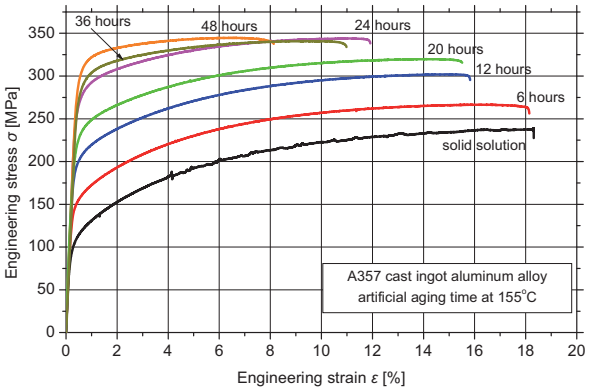

Fig. 1. Typical engineering stress – strain tensile flow curves of the A357 cast aluminum alloy for different artificial aging heat treatment times.

Typical three impact force – displacement curves of the investigated A357 alloy and for different artificial aging conditions can be seen in Figure 2. The points of impact yielding force F_{gy} (triangular points), maximum impact force F_m (circular points) and unstable crack propagation (square points) can be seen in the respective Figure as different points. In addition, absorbed impact energy W_{CVN} of each specimen can be seen in the right y-axis as a function of the hammer displacement during impact. All the above parameters are expected to vary with the different microstructural features of the alloy for its different artificial aging conditions.

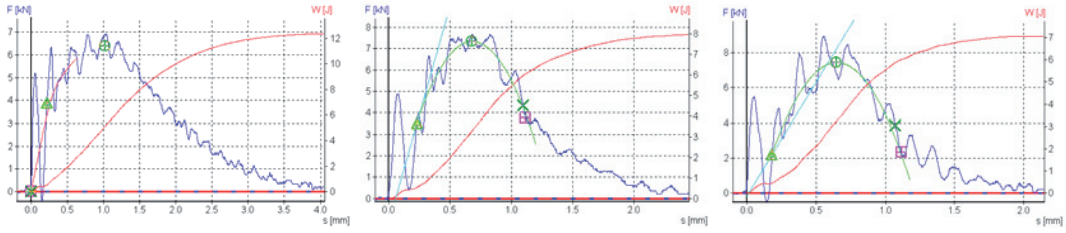

(a) (b) (c)

Fig. 2. Typical impact force – displacement curves of the investigated A357 cast aluminum alloy for (a) 6 hrs, (b) 24 hrs and (c) 48 hrs artificial aging time at 155°C.

Evaluated measurements of the impact yield force F_{gy} of the Charpy V-notch specimens for the different artificial aging conditions can be seen in Figure 3a. Artificial aging at 155°C shows that

there is a continuously increasing trend of F_{gy} with increasing aging time. Same is observed for the case of 175°C, where, as expected, this increase is more intense than the previous aging temperature. Aging at 205°C increases the yield force of the coupons up to the plateau of approximate 5 kN. As also discussed in [9,10], further aging at this temperature leads to overaging of the precipitates and an essential decrease in yield force is noticed. Figure 3b shows the respective yield strength results from the tensile tests. As can be noticed from comparison of the two Figures, the results from the different tests seem to have absolutely the same trend.

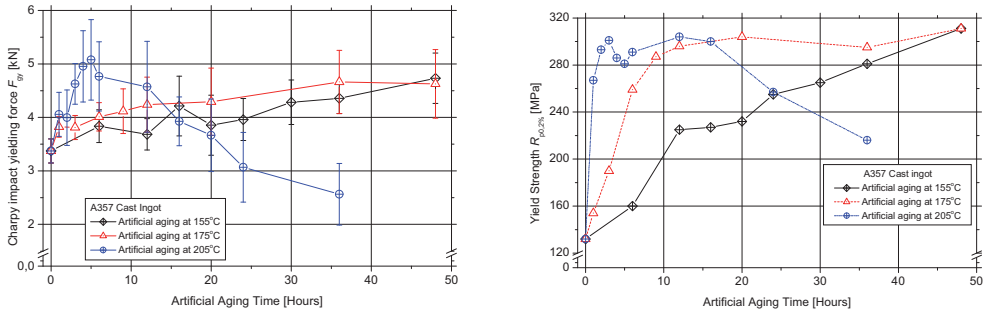

(a) (b)

Fig. 3. Effect of different artificial aging heat treatment conditions on (a) impact yielding force F_{gy} and (b) tensile yield strength $R_{p0.2\%}$ of the investigated A357 cast aluminum alloy.

The maximum impact force F_m of the Charpy V-notch specimens with varying artificial aging conditions can be seen in Figure 4. As expected, higher values of impact force were recorded than the respective impact yield forces. It seems that for all artificial aging temperatures, a maximum plateau of approximate 7.5 kN is reached. Overaging at 205°C leads to an essential decrease in F_m property. Identical results were noticed for the tensile tests; the tensile strength plateau is approximate 340 MPa, while overaging decreases the R_m property by almost 80 MPa for the case of 36 hours at 205°C.

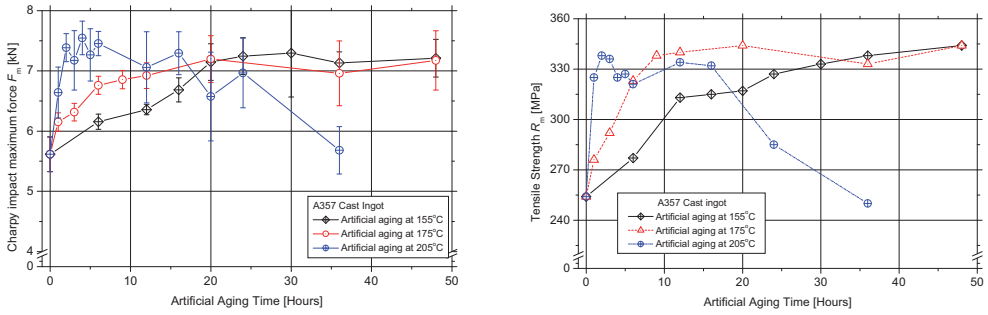

(a) (b)

Fig. 4. Effect of different artificial aging heat treatment conditions on (a) impact maximum force F_m and (b) tensile strength R_m of the investigated A357 cast aluminum alloy.

The Charpy V notch impact energy values W_{CVN} had been calculated as the integral below the impact force – displacement curves. In order to relate impact energy to the test specimen geometrical dimensions, material property values of impact resistance R_{CVN} were calculated. The term R_{CVN} was defined as:

$$R_{CVN} = \frac{W_{CVN}}{F_0}, \tag{2}$$

with F_0 being the reduced cross-section area of the impact specimen. The dependence of the impact resistance R_{CVN} on the aging time for the aging temperatures investigated can be seen in Figure 5a. The impact resistance decreases with increasing time from the initial value of 155 kJ/m^2 for the material before aging and tends to a value about 75 kJ/m^2 after artificial aging for peak tensile strength condition. The observed dependency of the impact resistance on the aging time correlates well to the decrease of tensile strain energy density W with increasing aging time (Figure 5b). It should be noticed that, as tensile strain energy density and impact resistance refer to mechanical load application rates that differ by more than five orders of magnitude, their direct correlation is not a straightforward issue.

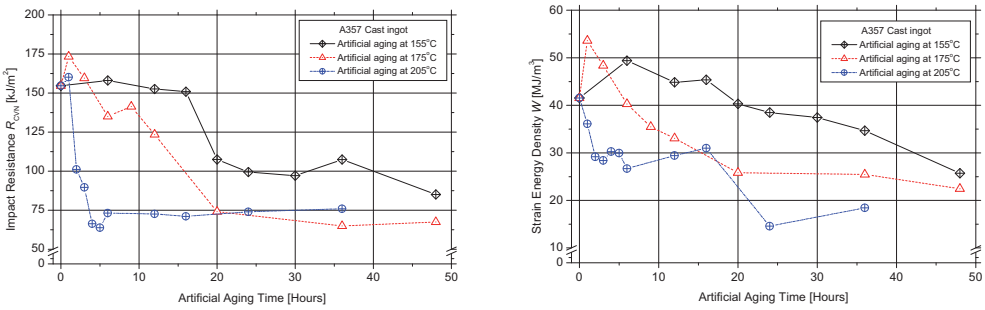

(a) (b)

Fig. 5. Effect of different artificial aging heat treatment conditions on (a) impact resistance R_{CVN} and (b) tensile strain energy density W of the investigated A357 cast aluminum alloy.

4 Analysis of the results

The strain energy density W can be evaluated from the area under the tensile stress – strain curve as:

$$W = \frac{dU}{dV} = \int_0^A \sigma \cdot d\varepsilon \tag{3}$$

where U is the strain energy V the material volume and A the elongation just before fracture. It is reported in the literature [10], that it can be roughly assessed by taking into account the yield strength R_p, tensile strength R_m, elongation to fracture A_f, or from even tensile strength and elongation to fracture.

Strain energy density W is a material property, which characterizes the damage tolerance potential of a material and may be used to evaluate the material fracture under both, static and fatigue loading conditions [6]. Note that energy density may be directly related to the plane strain fracture toughness value K_{Ic} [11,12], which evaluates the fracture of a cracked member under plain strain loading conditions. The quantity dU/dV in eqn.(3) tends to a critical value of energy density W_C as the elongation tends to the elongation A at failure time. According to the works in [11,12], the critical energy density function may be related to the energy density factor S:

$$\left(\frac{dU}{dV}\right) = \frac{S}{r} \to \frac{S_C}{r_C} \quad \text{at instability,} \qquad W_C = \frac{S_C}{r_C} \,. \tag{4}$$

Note that the plane strain fracture toughness value K_{Ic} gives S_C since:

$$S_c = \frac{(1+\nu)(1-2\cdot\nu)\cdot K_{Ic}^2}{2\cdot\pi\cdot E}, \tag{5}$$

in which ν and E are the Poisson's ratio and Young's modulus, respectively. The critical ligament size r_C measured from the crack tip is related to the process zone size that has been discussed extensively in the literature. Crack initiation is assumed to prevail when dU/dV $\to$ (dU/dV)$_C$ while the onset of rapid crack propagation is assumed to be reached when $S \to S_C$. Refer to [11,12] and the

references therein for more details, particularly the application of the energy density approach to ductile materials [6]. Substituting the critical energy factor S_C of eqn.(4) to eqn.(5), the material's plane strain fracture toughness becomes a function of the strain energy density:

$$K_{Ic}^2 = \frac{2 \cdot \pi \cdot E \cdot r_c \cdot W}{(1+\nu) \cdot (1-2 \cdot \nu)} \cdot \tag{6}$$

To this end, the values of fracture toughness K_{Ic}^2 and strain energy density W of the investigated cast aluminum alloys had been plotted in Figure 6. As can be seen, the pairs of their respective values can be linearly fitted with a good approximation (R^2 = 0.91). The pair of values (K_{Ic}^2,W) can be substituted to eqn.(6) and calculate the critical ligament r_C from the crack tip for each alloy, given that the Young's modulus E and the Poisson ratio ν values are the same for all the investigated materials. The calculation results can also be found in the same Figure, and the calculated ligaments ranged from 28 to 74 μm for the investigated alloys. As noticed in [13], this ligament size r_C is actually of the order of magnitude of the material's grain size.

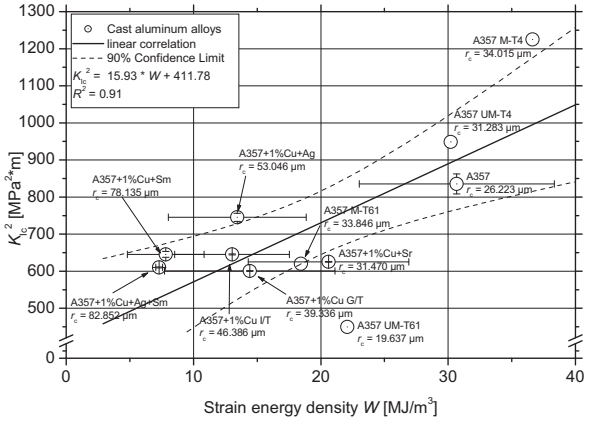

Fig. 6. Correlation between strain energy density W and square of plane strain fracture toughness K_{Ic}^2 values of A357 cast aluminium alloys [13].

The correlation of impact energy and tensile strain energy density has not been reported in the open literature. Yet, in the early 70's an empirical equation was proposed for both, low-alloyed and austenitic steels, to calculate the alloy's plane strain fracture toughness K_{Ic}, for known Charpy V-notch impact energy W_{CVN} and yield strength R_p values [5]. For these steel alloys, a linear correlation between the ratios $(K_{Ic}/R_p)^2$ and W_{CVN}/R_p was introduced. In analogy to the above observation, in Figure 7, the ratio W/R_p^2 has been displayed over the ratio R_{CVN}/R_p for the investigated 25 different artificial aging heat treatments of the A357 cast alloy. In the plot, the tensile energy density has been involved instead of the plane strain fracture toughness as according to above considerations, W can be considered proportional to K_{Ic}^2. The experimental results of Figure 7 may be fitted well by the linear expression:

$$\frac{W}{R_p^2} = f \cdot \frac{R_{CVN}}{R_p} + g \tag{7}$$

where f = 20,57·10^{-4} m^2/kJ and g = 2,86·10^{-4} MPa^{-1} are empirically derived material constants. The standard deviation factor R was calculated to be 0.96. Yet, given the scatter of the properties of cast alloys, the observed deviations are acceptable. With eqn.(7), the impact test may be exploited to get quantitative information about the material's tensile ductility and toughness.

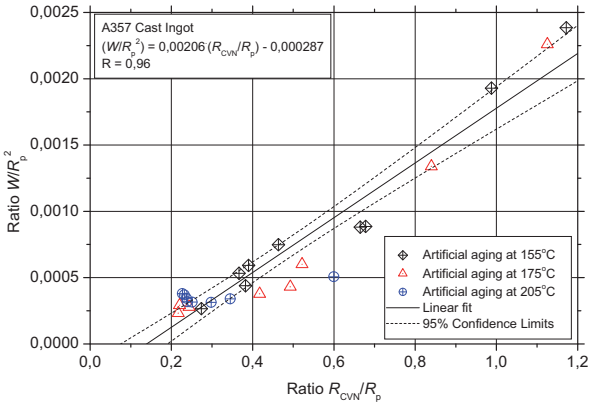

Fig. 7. Correlation of the plot of the ratio W/R_p^2 over R_{CVN}/R_p for the investigated artificial aging treatment conditions of the A357 cast aluminum alloy.

The performed fractographic analyses are supporting the physically arbitrary correlation of tensile strain energy density and impact resistance. Fracture surfaces from tensile and impact specimens obtained by using SEM are compared in Figures 8 and 9, respectively. The specimens in Figures 8a and 9a refer to solid solution, in Figures 8b and 9b to underaging (16 hours at 155°C), and in Figures 8c and 9c to peakaging conditions (16 hours at 205°C). For all aging conditions investigated, morphologically similar, rough fracture surfaces including large dimples were observed for the fractographs of the tensile specimens. These surfaces correspond to ductile fracture and imply the same void - coalescence fracture mechanism. As can be seen for the fracture surfaces of the impact specimens, the morphology of the fracture surfaces does not differ from the fracture surface morphology observed for the tensile specimens, despite the five order of magnitude difference in the rate of mechanical load application.

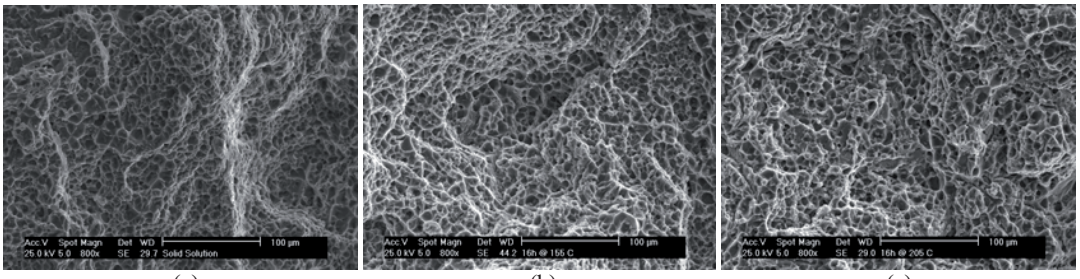

(a) (b) (c)

Fig. 8. Fracture surfaces of cast ingot A357 tensile specimens for (a) solid solution, (b) aging for 16 h at 155°C and (c) aging for 16 h at 205°C.

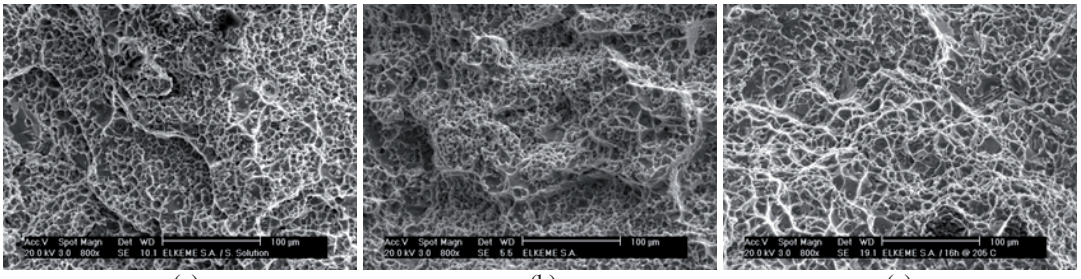

(a) (b) (c)

Fig. 9. Fracture surfaces of cast ingot A357 impact specimens for (a) solid solution, (b) aging for 16 h at 155°C and (c) aging for 16 h at 205°C.

In Figure 10, micrographs of the fracture surfaces of the impact specimens aged for 48 hours at 155°C and 16 hours at 205°C, respectively, are presented by involving a higher SEM resolution. In the Figures, additionally to the dimples, same micro-cracks may be observed as well. Using the EDX analysis, it was found that the cracked areas all over the specimen contain high Si quantities [10,13]. In the A357 alloy, high quantities of Si may be observed only in the Si particles; they are preferably located at the grain boundaries of the Al-phase. This observation is indicative for an intercrystalline fracture mode and is consistent to previous investigations [14,15].

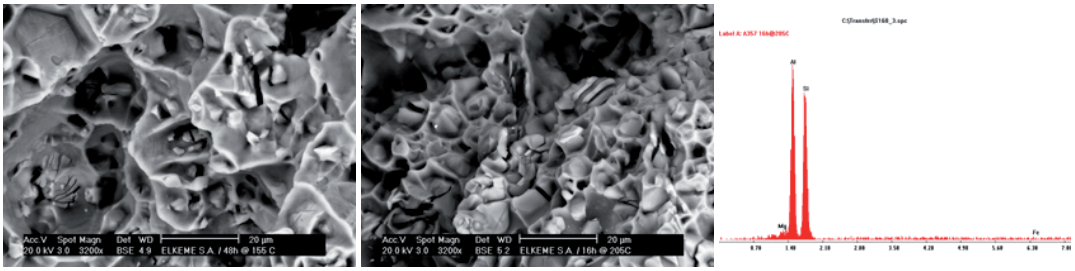

(a) (b) (c)

Fig. 10. Fracture surfaces of cast ingot A357 impact specimens for (a) aging for 48 h at 155°C, (b) aging for 16 h at 205°C and chemical analysis of the latter heat treatment condition.

References

1. M. Tiryakioğlu, J. Campbell, J.T. Staley, Scripta Mater., **49**, 873 (2003)
2. N.D. Alexopoulos, J. Mater. Eng. Perform., **15**, 59 (2006)
3. M. Tiryakioğlu, J. Campbell, N.D. Alexopoulos, Metall. Mater. Trans. B, **40B**, 810 (2009)
4. Anon. Advanced aluminum precision casting for integrally stiffened net shape components (ADVACAST). Final technical report of BRITE project 4084, Brussels, Belgium, (1996)
5. J. Barson and S. Rolfe: Impact Testing of Metals, ASTM STP 466, ASTM International, West Conshohocken, PA, pp. 281–302 (1970)
6. D. Yeong, O. Orringen, G Sih, J. Theor. Appl. Fract. Mech., **22**, 127 (1995)
7. D. Apelian, S. Shivkumar, G. Sigworth, AFS Trans., **137**, 727 (1989)
8. J.R. Davis, editor. ASM Specialty Handbook: Aluminum and Aluminum Alloys. ASM International, Metals Park, Ohaio, USA, (1993)
9. N.D. Alexopoulos, Sp.G. Pantelakis, Mater. Des., **25**, 419 (2004)
10. N.D. Alexopoulos, Sp.G. Pantelakis, Metall. Mater. Trans. A, **35A**, 3079 (2004)
11. G. Sih, C. Chao, J. Theor. Appl. Fract. Mech., **2**, 67 (1984)
12. G. Sih, D. Yeong, J. Theor. Appl. Fract. Mech., **14**, 141 (1990)
13. N.D. Alexopoulos, M. Tiryakioğlu, Metall. Mater. Trans. A, **40A**, 716 (2009)
14. L. Zhen, S.B. Kang, Metall. Mater. Trans. A, **28A**, 1489 (1997)
15. Q.G. Wang, S.B. Kang, Mat. Sci. and Eng. A, **A241**, 72 (1998)